



Two point Josephson junctions in a superconducting stripline: static case

J.-G. Caputo^{a,b,*}, Y. Gaididei^c

^a *Laboratoire de Mathématiques, INSA de Rouen, Boite Postale 8, 76131 Mont-Saint-Aignan Cedex, France*

^b *Laboratoire de Physique Théorique et Modélisation, Université de Cergy-Pontoise and C.N.R.S., 95031 Cergy-Pontoise Cedex, France*

^c *Bogoliubov Institute of Theoretical Physics, Academy of Sciences of Ukraine, 252143 Kiev, Ukraine*

Received 6 May 2003; received in revised form 11 September 2003; accepted 23 September 2003

Abstract

We consider the static behavior and maximum critical current $I_{\max}(H)$ for a given magnetic field H of a system of two point Josephson junctions separated by a distance $2a$ embedded in a rectangular microstrip of width w and show that the problem can be mapped onto an effective 1D situation with a rescaled width $\bar{w} < w$ which depends on the geometrical parameters a , w and mis-alignment b of the junction pair. The analysis of the reduced equations reveals that I_{\max} is periodic of period $\frac{\pi}{a}$ and yields the amplitude of its variation with the magnetic field H . In particular it is proportional to $\frac{a}{w}$ when $a < w$ and is reduced when the mis-alignment b is increased. Since the geometric parameters can be freely chosen in the fabrication process we suggest that experimentalists can design a device to suit specific needs.

© 2003 Elsevier B.V. All rights reserved.

PACS: 85.25.Cp; 74.50.+r; 75.80

1. Introduction

Josephson junctions are weak links between two superconductors. The current of pairs I_J and the voltage V between the two superconductors are given to a very good approximation by the two Josephson relations $\sin(\phi) = I_J$ and $\frac{d\phi}{dt} = V$, where ϕ is the phase difference between the two metal

layers [1]. The electrodynamics of such systems is based on the couple (charge, phase) contrary to the classical (current, voltage) one and is described by an sine-Gordon equation for ϕ where the space unit is the Josephson length λ_J [2]. Such a model can be generalized to the case when the current density is inhomogeneous or when several junctions exist between the two superconductors. Both situations lead to an inhomogeneous sine-Gordon equation which exhibits interesting linear–nonlinear couplings [3,4].

In the static regime $V \equiv 0$ Josephson junctions oppose an external magnetic field by generating a current. Experimentalists measure the maximum current $I_{\max}(H)$ for a given magnetic field H and

* Corresponding author. Address: Laboratoire de Mathématiques, INSA de Rouen, Boite Postale 8, 76131 Mont-Saint-Aignan Cedex, France. Tel.: +33-235-5283-44; fax: +33-235-5283-32.

E-mail addresses: caputo@insa-rouen.fr (J.-G. Caputo), yugaid@bitp.kiev.ua (Y. Gaididei).

this gives an indication of the quality of the junction and also some information about its features. This behavior leads to a well-known application of these devices to the measure of magnetic fields, using two junctions of size smaller than λ_J in a SQUID arrangement. When the junction has length much longer than λ_J , the junction screens the applied magnetic field and one obtains the characteristic piecewise linear pattern first analyzed by Owen and Scalapino [5].

In the inhomogeneous case it is difficult to relate $I_{\max}(H)$ to geometrical properties of the device when the current density is variable or in the 2D case when several junctions are present in a microstrip. Inhomogeneities only affect $I_{\max}(H)$ when they are within $2\lambda_J$ of the boundaries as shown in the 1D study of Chow et al. [6] who simulated using a mechanical analog regions of low critical current density in a long Josephson junction. These results can be related to the analysis of Gal'pern and Filippov [7]. This study is also important from a fundamental point of view because high T_c superconductors are polycrystals and grain boundaries cause random variations of the critical current density. Fehrenbacher et al. [8] examine the cases of periodic and random distributions of defects.

Here we consider the case when several junctions are present in a 2D microstrip. Then $I_{\max}(H)$ is bounded by the total area of the junctions but one would like a sharper estimate depending on the magnetic field. This is difficult both due to the Neumann boundary conditions and the periodic nonlinearity [9]. A simpler configuration is when a single rectangular junction is surrounded by a fairly small passive region where no tunneling occurs. This has the two advantages of shielding the delicate oxide layer from the environment and allowing a good electromagnetic coupling to a superconducting line, a useful feature when using the junction in a complex device like a radioastronomy receiver. For this window configuration where a junction of width w is surrounded by a passive region of extension w' one of us showed using a variational approach that the characteristic length scale becomes [10] $\lambda_{\text{eff}} = \lambda_J \sqrt{1 + 2\frac{w'}{w}} > \lambda_J$ so that long junctions become shorter due to the passive region. This result was confirmed experimentally

[11] yielding a correct estimate of the minimum magnetic field giving a zero current.

The situation is more complex when several Josephson junctions are present in a passive region because of the global coupling between them due to the Laplacian operator, also the alignment of the junctions with the applied magnetic field becomes important. In the present study we want to understand these effects on a simple model of two small strip Josephson junctions placed in a cavity. In addition to being a SQUID such a system is also routinely used as a wave mixer for radiofrequency detection in radioastronomy [12]. We have studied in detail the static behavior and obtained the following main features of the maximum current $I_{\max}(H)$:

- $I_{\max}(H)$ is periodic of period H_c and amplitude A_I which we determine. In particular $H_c = \frac{\pi}{2a}$ where $2a$ is the distance between the two junctions.
- The 2D problem can be mapped into a 1D effective problem of reduced width $\bar{w} > w$, a result connected to the rescaling of λ_J into λ_{eff} for long junctions in a microstrip.

These features show that one can tailor the $I_{\max}(H)$ curve to suit specific needs and in particular obtain maximum sensitivity for specific values of the field.

The paper is organized as follows: Section 2 describes the 2D model and its reduction to an effective 1D system, the details of which are given in Appendix A. In Section 3 we study the 1D effective model and show how to obtain $I_{\max}(H)$. Section 4 presents and analyses numerical results for different configurations and Section 5 is our conclusion.

2. The 2D model

We consider the static behavior of a two-dimensional Josephson device which consists of two superconducting metal plates (parallel to the x - y plane) separated by an inhomogeneous thin oxide layer as shown in Fig. 1. The electromagnetic behavior of such a system is governed by

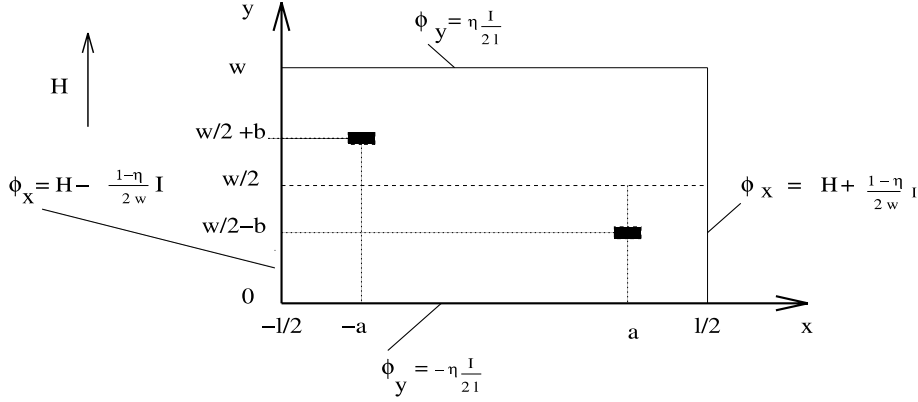


Fig. 1. Plot of the microstrip containing the two point Josephson junctions. The extension of the junctions along the x axis is d . The total current I applied to the device has an overlap component η and an inline component $1 - \eta$ where $0 < \eta < 1$.

Maxwell's equations coupled with the Josephson equation

$$J_z(x, y) = J_0(x, y) \sin(\phi) \quad (1)$$

for the tunneling supercurrent density through the oxide layer. In Eq. (1) $\phi(x, y)$ is the difference of the phases of the order parameters in the two superconductors and $J_0(x, y)$ is the inhomogeneous maximum critical current density.

Here we will study the particular case of two small junctions located in a rectangular microstrip of length l and width w at the positions $(a, w/2 - b)$ and $(-a, w/2 + b)$ where the coordinate system (x, y) is such that $-l/2 \leq x \leq l/2$ and $0 \leq y \leq w$ (see Fig. 1). Following previous studies on window Josephson junctions [3], the phase difference $\phi(x, y)$ for this system is then given by

$$\Delta\phi = \left[\delta \left(y - \left(\frac{w}{2} - b \right) \right) g(x - a) + \delta \left(y - \left(\frac{w}{2} + b \right) \right) g(x + a) \right] \sin(\phi), \quad (2)$$

where Δ is the two-dimensional Laplacian, the spatial dimensions are in units of λ_J , δ is the usual Dirac delta function and $g(x) = (\sqrt{\pi}d)^{-1} \exp(-x^2/d^2)$ where the parameter $d \ll l$ is the width of the junction along x . We used this model to avoid the well-known singularity at the origin of the Green's function for the Laplacian operator in 2D. Also note that in the experiments of [12], the ratios $d/l \approx 10^{-2}$ and $d/w \approx 10^{-1}$.

The boundary conditions of mixed type on the normal derivatives on the domain boundary $\partial\Omega$ are given by [2]

$$\vec{n} \nabla \phi|_{\partial\Omega} = \vec{n} \cdot (\vec{z} \times \vec{H})_{\partial\Omega}, \quad (3)$$

where \vec{n} is the exterior normal, \vec{z} the unit vector along the z -direction (so that (x, y, z) is direct) and \vec{H} is the magnetic field directly applied or created by the applied current. We will normalize the magnetic field and currents. In the case of a magnetic field of amplitude H parallel to the y axis, the boundary conditions (3) can be written, using ∂ to denote partial derivatives

$$\begin{aligned} \partial_y \phi|_{y=0} &= -\frac{I}{2l} \eta, \\ \partial_y \phi|_{y=w} &= \frac{I}{2l} \eta, \\ \partial_x \phi|_{x=\pm l/2} &= H \pm \frac{I}{2w} (1 - \eta), \end{aligned} \quad (4)$$

where we have a mixed current feed with an inline component $(1 - \eta)I$ and an overlap component ηI where $0 < \eta < 1$ so that the total dc current I going through the device

$$\int_{-l/2}^{l/2} dx \sin(\phi) = I.$$

Before presenting the reduction of the problem to a 1D effective one, several remarks are useful. In the simplest case where there is only one junction

in the domain, a simple calculation shows that for any value of the current below the critical value ($= 1$), once H is fixed, there is always a solution. Then the maximum current is always reached so that $I_{\max} = 1$ independently of H . This is consistent with the usual $\frac{\sin(\pi H/H_c)}{H}$ interference type pattern observed in experiments for small Josephson junctions for which $H_c \propto 1/d$ where d is the junction extension [13] because here we assume $d \ll 1$ so that $H_c \gg 1$. When other junctions are present in the microstrip more length scales are introduced and the model is very useful to describe their coupling.

Secondly remark that the system is invariant under the following transformation

$$x' = -x, \quad \phi' = -\phi, \quad I' = -I, \quad (5)$$

so that for a given magnetic field H , a solution for a given $I > 0$ will yield a solution for $I < 0$ obtained through the above given transformation.

In a first step we reduce the problem to homogeneous Neumann boundary conditions by making the change of field

$$\phi(x, y) = \frac{I\eta}{2lw} \left(y - \frac{w}{2} \right)^2 + \psi(x, y), \quad (6)$$

so that ψ can be expanded in a cosine Fourier series in y

$$\begin{aligned} \psi(x, y) &= A_0(x) + \sum_{m=1}^{\infty} A_m(x) \cos\left(\frac{m\pi y}{w}\right) \\ &\equiv A_0 + B. \end{aligned} \quad (7)$$

Introducing (6) and (7) into (2) we obtain

$$\begin{aligned} \Delta\psi &= \left[\delta \left(y - \left(\frac{w}{2} - b \right) \right) g(x-a) \sin(C + A_0 + B_-) \right. \\ &\quad \left. + \delta \left(y - \left(\frac{w}{2} + b \right) \right) g(x+a) \sin(C + A_0 + B_+) \right] \\ &\quad - \eta \frac{I}{s}, \end{aligned} \quad (8)$$

where $s = lw$ is the total area of the device, $C = \eta \frac{b^2}{2} \frac{l}{s}$,

$$\begin{aligned} B_- &\equiv B \left(x, y = \frac{w}{2} - b \right) \\ &= \sum_{m=1}^{\infty} A_m \cos \left[\frac{m\pi}{w} \left(\frac{w}{2} - b \right) \right], \end{aligned} \quad (9)$$

and

$$\begin{aligned} B_+ &\equiv B \left(x, y = \frac{w}{2} + b \right) \\ &= \sum_{m=1}^{\infty} A_m \cos \left[\frac{m\pi}{w} \left(\frac{w}{2} + b \right) \right]. \end{aligned} \quad (10)$$

To simplify the notation we define $\gamma = 2\pi/w$ and $m_{\pm} = \frac{m\pi}{w} \left(\frac{w}{2} \pm b \right)$.

We can then project Eq. (8) on the different modes A_m in the y -direction, to obtain

$$\begin{aligned} \partial_x^2 A_0 &= \frac{1}{w} [g(x-a) \sin(C + A_0 + B_-) \\ &\quad + g(x+a) \sin(C + A_0 + B_+)] - \eta \frac{I}{s}, \end{aligned} \quad (11)$$

with boundary conditions $\partial_x A_0|_{x=\pm \frac{l}{2}} = H \pm (1 - \eta) \frac{l}{2w}$. The amplitudes A_m of the transverse modes for $m > 1$ satisfy

$$\begin{aligned} \partial_x^2 A_m - \left(\frac{\gamma m}{2} \right)^2 A_m \\ &= \frac{2}{w} [\cos(m_-)g(x-a) \sin(C + A_0 + B_-) \\ &\quad + \cos(m_+)g(x+a) \sin(C + A_0 + B_+)], \end{aligned} \quad (12)$$

with homogeneous Neumann boundary conditions.

We now proceed to solve formally the equation for A_m , $m > 1$, compute the terms C , B_- and B_+ and reinject them into the equation for A_0 to get a self-consistent equation for $A = A_0 + C$. This equation can be solved formally and this calculation is given in detail in Appendix A so that we present directly the end result in terms of two parameters α and β

$$\begin{aligned} I &= 2 \sin(\alpha) \cos(\beta a), \\ H - \beta &= \frac{1}{w} \cos(\alpha) \sin(\beta a), \end{aligned} \quad (13)$$

where

$$\bar{w} = \frac{w}{k}; \quad k = 1 + \frac{w}{2\pi a} [p - q(a)] \quad (14)$$

and the values of p and $q(a)$ as calculated in Appendix B are

$$p \approx \frac{1}{2}C + \frac{\sqrt{\pi d}}{w} + \log \frac{w}{\pi d} - \log \left(\cos \frac{\pi b}{w} \right), \quad (15)$$

$$q(a) = -\log(1 + e^{-\gamma a}) - \frac{1}{2} \log[1 - 2e^{-\gamma a} \cos(\gamma b) + e^{-2\gamma a}]. \quad (16)$$

Apart from this rescaling of w this algebraic system is identical to the one that would be obtained by solving the 1D effective problem

$$w \partial_x^2 A = \delta(x-a) \sin A + \delta(x+a) \sin A - \eta \frac{I}{l}, \quad (17)$$

with

$$A_x = H \pm (1 - \eta) \frac{I}{2w} \quad \text{for } x = \pm \frac{l}{2}.$$

A confirmation of this fact is that in the limit of a very small width w of the passive region p , $q(a) \rightarrow 0$ so that $B_-(a)$ and $B_+(-a)$ vanish. The equation for $A = A_0 + C$ obtained from (11) then reduces to (17). From this one sees that the two-dimensional character of the problem appears in k . We will analyze this factor in Section 4 but first we give the solution of (13).

3. Analysis of the one-dimensional effective model

We rewrite (13) as

$$\sin(\alpha) \cos(z) = I/2, \quad (18)$$

$$\cos(\alpha) \sin(z) = w \left(H - \frac{z}{a} \right), \quad (19)$$

where $z = \beta a$ and we have omitted the bar in w .

We use this system to compute the solution (α, z) for a given magnetic field H and current I . First notice that for I fixed, the solution is periodic in H of period $\frac{\pi}{a}$ because the system is invariant under the transformation

$$H' = H - \frac{n\pi}{a}, \quad z' = z - n\pi, \quad \alpha' = \alpha - n\pi. \quad (20)$$

It is not surprising that we find this periodic behavior since this system is essentially a SQUID [13].

For the analysis, due to the above mentioned symmetries we restrict ourselves to the subset of parameter space $0 \leq H \leq \frac{\pi}{a}$ and $0 \leq z \leq \pi$. If $0 < \alpha < \pi$ then we can write

$$\frac{I}{2} = \cos(z) \sqrt{1 - \frac{\left(\frac{z}{a} - H\right)^2}{\sin^2(z)}} w^2 < |\cos z|. \quad (21)$$

Let us now fix H . There is a solution if $1 - \frac{\left(\frac{z}{a} - H\right)^2}{\sin^2(z)} w^2 \geq 0$ so if $0 \leq z \leq \pi$ then z verifies $H_-(z) \leq H \leq H_+(z)$ where $H_{\pm}(z) = \frac{z}{a} \pm \frac{\sin(z)}{w}$.

To analyze this in detail we have plotted in Fig. 2 the two curves $H_{\pm}(z)$ for three values of the junction spacing $a = 0.2, 1$ and 2 , from left to right. For a given H the values of z that are admissible lie in the interval between the two curves. The value $z_m = Ha$ gives the upper bound of the current $I_{\max} = I(z_m) = 2 \cos(Ha)$. The function $|\cos(z)|$ is plotted to show that one should expect

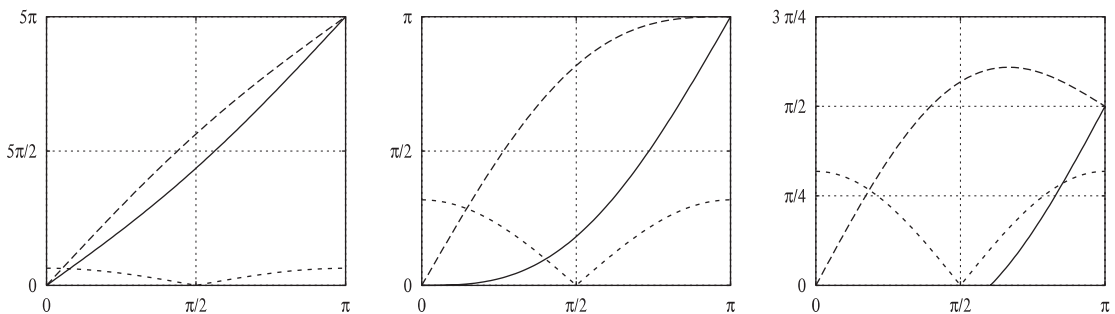


Fig. 2. Plot of the functions $H_{\pm}(z) = z/a \pm \sin(z)/w$ for three different spacings of the point junctions, $a = 0.2, 1, 2$ from left to right. The function $|\cos(z)|$ is shown in small dashed line. The parameter $w = 1$.

to find a large value of the maximum (positive) current for z close to 0, π and a small value of the maximum (positive) current for $z \approx \pi/2$. For $a = 0.2$ shown in the left panel of Fig. 2, $\frac{z}{a} \gg \sin(z)$ so that for a given H there is a very narrow interval of possible values of z so that $z \approx aH$ and $I \approx 2 \times \cos(aH)$ whose absolute value is minimum for $H = \pi/(2a)$. On the contrary for $a = 1$ and 2 (middle and right panels of Fig. 2) the range of possible values of z is much larger and there is no longer a simple estimate for I . For these large values of a one then expects the minimum of $|I|$ to be larger than for $a = 0.2$.

In order to validate the simple model (17) it is important to compare its solutions with the experimental results [12]. Therefore we now consider the practical evaluation of $I_{\max}(H)$, the maximum current I for which a solution of (17) exists for a given magnetic field. We start from (18) and eliminate α to obtain the following transcendent equation:

$$\left(\frac{I}{2}\right)^2 \frac{1}{(\cos z)^2} + w^2 \left(H - \frac{z}{a}\right)^2 \frac{1}{(\sin z)^2} - 1 = 0. \tag{22}$$

The range of z where one should look for solutions of (22) is given by the solvability condition for the two equations describing the jump of the derivative at the junctions (A.8) i.e.

$$-\frac{1}{w} \leq H + \frac{I}{2w} - \frac{z}{a} \leq \frac{1}{w},$$

$$-\frac{1}{w} \leq H - \frac{I}{2w} - \frac{z}{a} \leq \frac{1}{w}.$$

For $I > 0$ this yields an admissible range $z_{\min} < z < z_{\max}$, $z_{\min} = H + \frac{I}{2w} - \frac{1}{w}$ and $z_{\max} = H - \frac{I}{2w} + \frac{1}{w}$, where a solution of (22) yields a solution of the full problem. The procedure to obtain the maximum current I_{\max} for a given magnetic field H is

```

for I = 0, 2, dI
  compute  $z_{\min} z_{\max}$ 
  for  $z_{\min} < z < z_{\max}$ , solve (22) and compute
   $I_c =$  maximum of  $I$ 
  write  $H, I_c$ 
end
    
```

We report in Fig. 3 the computed $I_{\max}(H)$ for $a = 0.2$. As expected the plot is periodic of period π/a . For $a = 1, 2$ and 3, the curves $I_{\max}(H)$ shown in Fig. 4 show again a periodicity of period π/a . As expected the minimum of the critical current increases if the distance between the two junctions is increased. When $a \rightarrow +\infty$ we recover the one junction case for which I_{\max} is constant ($= 1$).

In fact one can estimate the minimum of the critical current as a function of a . First note that for a given H the extrema of the current $I(z, H)$ defined by Eq. (21) are determined by $\frac{\partial I}{\partial z} = 0$. This

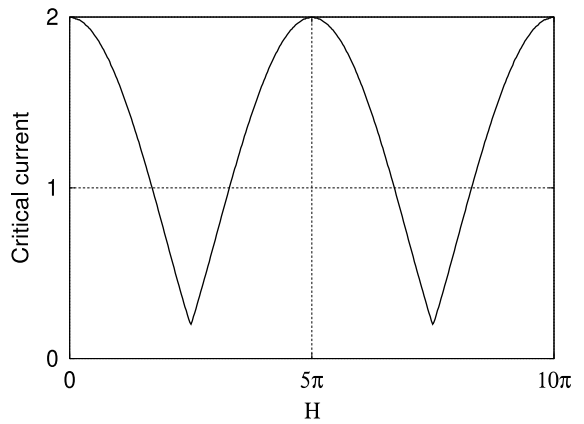


Fig. 3. Critical current vs. H for $a = 0.2$. The parameter $w = 1$.

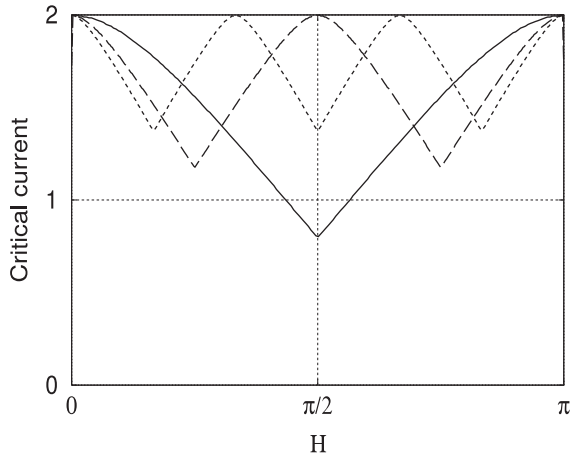


Fig. 4. Critical current vs. H for $a = 1$ in full line, $a = 2$ in long dash and $a = 3$ in short dash. The parameter $w = 1$.

relation is verified for the following two values of H

$$H = H_1(z) \equiv \frac{z}{a} - \frac{1}{2a} \left(\cos z - \sqrt{\cos^2 z + 4 \frac{a^2}{w^2} \sin^2 z} \right) \sin z, \quad (23)$$

$$H = H_2(z) \equiv \frac{z}{a} - \frac{1}{2a} \left(\cos z + \sqrt{\cos^2 z + 4 \frac{a^2}{w^2} \sin^2 z} \right) \sin z. \quad (24)$$

The corresponding extrema values of the current $I(z, H)$ are given by

$$I_1(z_1, H) = 2 \cos z_1 \times \sqrt{1 - \frac{w^2}{4a^2} \left(\cos z_1 - \sqrt{\cos^2 z_1 + 4 \frac{a^2}{w^2} \sin^2 z_1} \right)^2},$$

$$I_2(z_2, H) = 2 \cos z_2 \times \sqrt{1 - \frac{w^2}{4a^2} \left(\cos z_2 - \sqrt{\cos^2 z_2 + 4 \frac{a^2}{w^2} \sin^2 z_2} \right)^2}, \quad (25)$$

where $z_1(z_2)$ is the root of Eq. (23) (Eq. (24)), respectively. Both z_1 and z_2 provide maxima for $|I(z, H)|$ because $I_1(z_1, H)I_2(z_2, H) < 0$. The maximal current depends on the magnetic field H and reaches a minimum for $H = H_c$ when the two extrema $I_1(z_1, H)$, $I_2(z_2, H)$ are equal and opposite. This effect is illustrated by Fig. 5 which shows $I(z, H)$ as a function of z for $H < H_c$, $H = H_c$ and $H > H_c$. The value of H for which the critical current is minimum corresponds to $I_1 = -I_2$ and the minimum value of the critical current is determined by the equations:

$$H_1(z_1) = H_2(z_2), \quad (26)$$

$$|I_1(z_1, H)| = |I_2(z_2, H)|. \quad (27)$$

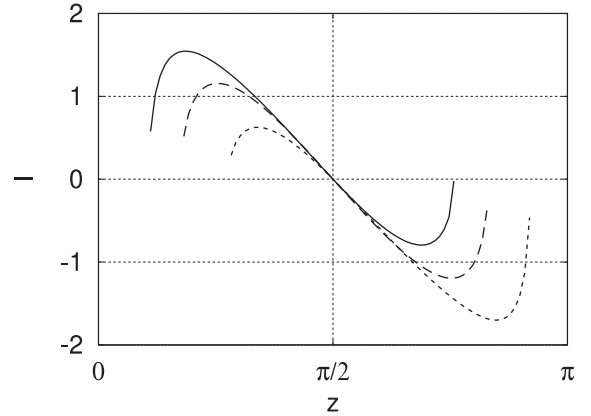


Fig. 5. Plot of the current $I(z)$ for $a = 2$ and $H = 0.5$ (continuous line), $H = 0.8$ (long dashed line) and $H = 1.2$ (short dashed line). The parameter $w = 1$.

It is seen from (27) that $z_2 = \pi - z_1$ and from (26) we get $H_m = \pi/2a$ and the value of the minimum critical current is determined by the relations

$$I_{\min} = 2 \cos z \sqrt{1 - \frac{w^2}{4a^2} \frac{(2z - \pi)^2}{\sin^2 z}}, \quad (28)$$

$$(2z - \pi)^2 - (2z - \pi) \sin 2z - 4 \frac{a^2}{w^2} \sin^4 z = 0.$$

The analysis of the function defining z indicates that there are two roots located on each side of $\pi/2$ and that the minimum critical current corresponds to the root on the left of $\pi/2$. The roots are close to $\pi/2$ for a/w not too large. In that case we write $2z - \pi = x$ and obtain using a Taylor expansion in x , $x_{\min} \approx \sqrt{\frac{2a^2}{a^2 + w^2}}$ so that the minimum critical current is

$$I_{\min} \approx x \left(1 - \frac{x^2}{8} \left(\frac{a^2}{w^2 + \frac{1}{3}} \right) \right) = \sqrt{\frac{2a^2}{a^2 + w^2}} \left(1 - \frac{1}{4} \frac{\frac{a^2}{3w^2} + 1}{\frac{a^2}{w^2} + 1} \right). \quad (29)$$

We have computed exactly the minimum critical current as a function of a/w and it is shown in Fig. 6. Notice that it increases quickly with a/w and that its initial slope is 1. The approximation (29) is also shown on this figure and is fairly close to the exact curve.

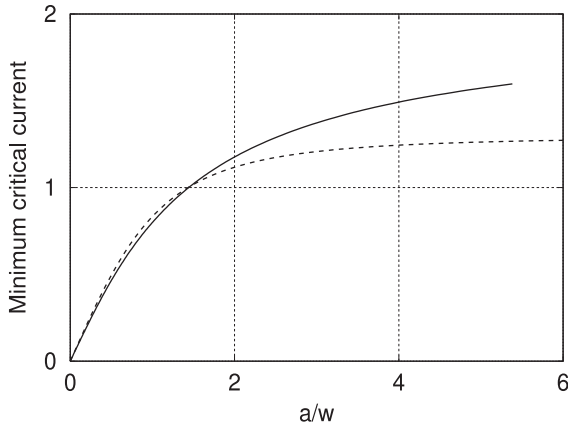


Fig. 6. Minimum of critical current as a function of a/w . The approximation (29) is shown in dashed line.

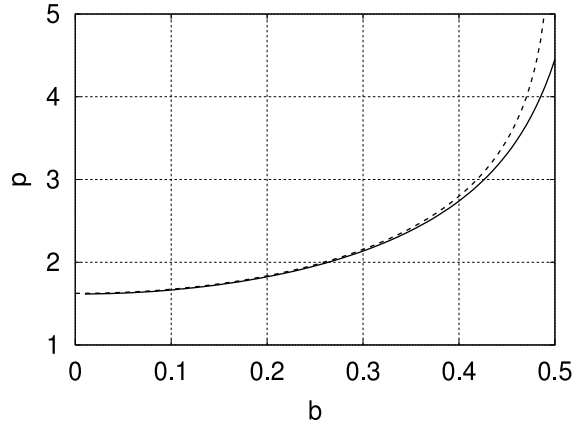


Fig. 7. Plot of $p(b)$ in full line, the approximation is shown in dashed line. The parameters $w = 1$ and $d = 0.1$.

4. Results and discussion

We have shown in Section 2 that the two-dimensional character of the problem appears through the effective width \bar{w} and rescaling coefficient k

$$\bar{w} = \frac{w}{k}; \quad k = 1 + \frac{w}{2\pi a} [p - q(a)]. \quad (30)$$

This does not affect the period of the curve $I_{\max}(H)$ which is completely determined by a as π/a .

To understand how k depends on the geometrical parameters of the problem w, a and b it is useful to consider its components p and $q(a)$. The term

$$p \approx \frac{1}{2}C + \frac{\sqrt{\pi}d}{w} + \log \frac{w}{\pi d} - \log \left(\cos \frac{\pi b}{w} \right), \quad (31)$$

is independent of a and is always positive. It is an on-site term which only depends on b and d . As such it diverges for $d \rightarrow 0$ as the log, this is the divergence of the 2D Green's function. Notice also that p increases with b and gets large only close to $b = w/2$ as shown in Fig. 7 (the divergence observed in the approximation for $b = w/2$ is artificial).

The component

$$q(a) = -\log(1 + e^{-\gamma a}) - \frac{1}{2} \log[1 - 2e^{-\gamma a} \cos(\gamma b) + e^{-2\gamma a}]$$

describes coupling between sites. The left panel of Fig. 8 shows that it decreases very fast with a/w and that it changes sign for a small b . As expected it diverges for $b = 0$ and $a \rightarrow 0$ as shown on the right panel of Fig. 8 and we recover the divergence of the 2D Green's function. Fig. 8 also shows that the dependence of q on b becomes very weak as soon as $a/w \geq 0.2$. In the difference $p - q(a)$ the first term dominates except when $a/w \ll 1$ so that $k > 1$. This means that $\bar{w} < w$ so that the 2D problem is equivalent to a 1D effective problem with a reduced width.

Let us now analyze specifically k as a function of w, a and b . First assume that the junctions are aligned with the magnetic field H so that $b = 0$. We see in Fig. 9 that k increases fast with w for a small due to the combined effect of the increase of p and decrease of $q(a)$. On the contrary for $a \geq 1$ the change in k remains very small.

To summarize, for small w k does not depend very much on a and is close to 1 so that $\bar{w} \approx w$. On the other hand when w is large, k is quite large for $a = 0.2$ ($\bar{w} < w$) and remains of order 1 for $a \geq 1$ ($\bar{w} \approx w$). This can be interpreted physically in the following way. If $w \ll 1$ only the fundamental transversal mode contributes to the solution and the coupling between junctions is essentially one dimensional. In the opposite case $w > 1$, many transversal modes contribute to the coupling between junctions, their number depends on a and w

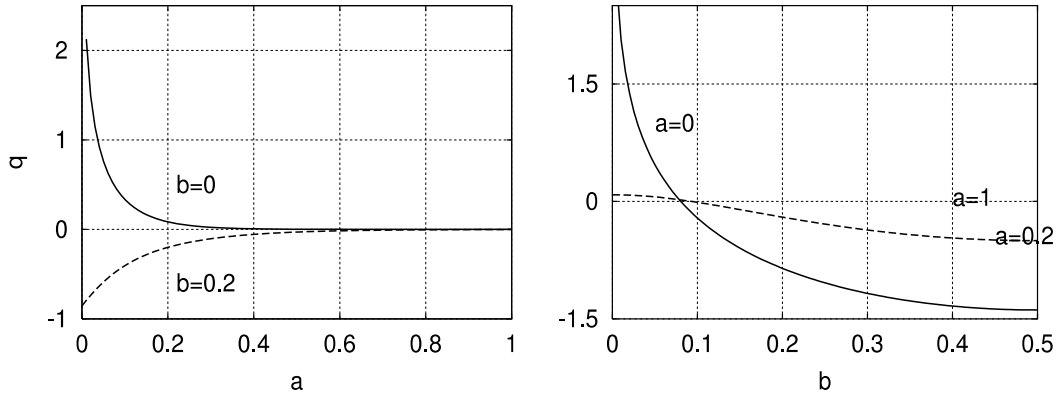


Fig. 8. Behavior of q vs. a and b . The left panel shows $q(a)$ for $b = 0$ and 0.2 , while the right panel shows $q(b)$ for $a = 0, 0.2$ and 1 . The parameter $w = 1$.

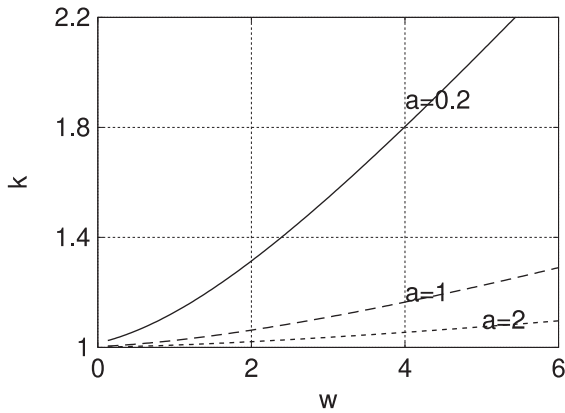


Fig. 9. Plot of the 2D rescaling coefficient $k = 1 + w[p - q(a)] / (2\pi a)$ vs. w for $a = 0.2, 1$ and 2 . The parameters $d = 0.1$ and $b = 0$.

making the problem essentially two dimensional. As a consequence for w small $\bar{w} \approx w$ independently of a so that we expect the minimum critical current to behave as in Fig. 6 and show a saturation as soon as $a/w \geq 2$. On the contrary for large w and small a , take for example $w = 5$ and $a = 0.2$ we get $k \approx 2$, $\bar{w} = 2.5$ and $a/\bar{w} = 0.08$ therefore the minimum critical current should then be much smaller than it was for $w = 0.2$. This effect can be seen immediately by comparing the left panels of Figs. 10 and 11 which show $I_{\max}(H)$ respectively for $w = 0.2$ and 5 for $a = 0.2$ (left panel), 1 (right panel) and 2 (right panel). As expected from Fig. 6 for $w = 0.2$ as shown in Fig. 10 the minimum critical current increases strongly as a increases from 0.2 to 1 and saturates. On the contrary for

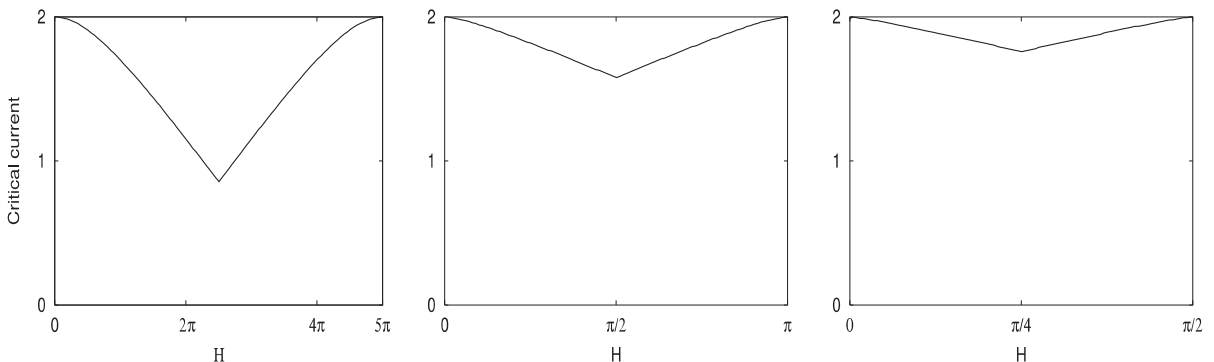


Fig. 10. Plot of $I_{\max}(H)$ for a small width of the passive region $w = 0.2$ and three values of a , $a = 0.2$ (left panel), $a = 1$ (middle panel) and $a = 2$ (right panel). The parameter $d = 0.1$.

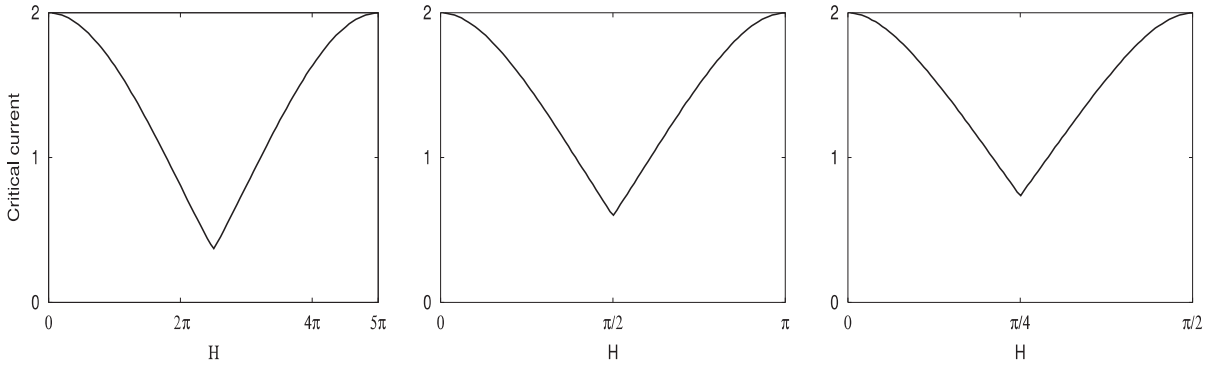


Fig. 11. Plot of $I_{\max}(H)$ for a large width of the passive region $w = 5$ and three values of a , $a = 0.2$ (left panel), $a = 1$ (middle panel) and $a = 2$ (right panel). The parameter $d = 0.1$.

$w = 5$ shown in Fig. 11 the minimum critical current increases monotonically as a increases from 0.2 to 1 and 2.

Now let us consider the case when $b > 0$. Fig. 12 shows k as a function of b for $a = 0.2, 1$ and 2 . Due to the behavior of p , k is the largest for $b = w/2$ and this value increases as a decreases so that $\bar{w} < w$ for $a = 0.2$ while $\bar{w} \approx w$ for $a \geq 1$. As seen in Fig. 12 for $a = 0.2$ k is much larger than for $a = 1$ and 2 . We therefore expect that for $a = 0.2$, \bar{w} will decrease faster than for $a = 2$, as b increases. Fig. 13 presents $I_{\max}(H)$ for $b = 0, 1$ and 2 for a large passive region $w = 5$ and $a = 0.2$ (left panel) and 2 (right panel). As expected for $a = 0.2$ the minimum critical current increases monotonically with b while for

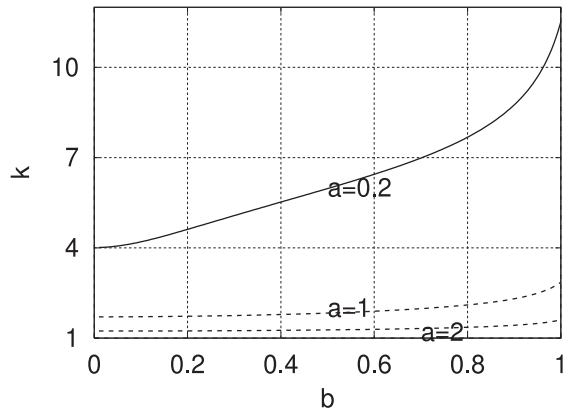


Fig. 12. Plot of the 2D rescaling coefficient $k = 1 + w[p - q(a)] / (2\pi a)$ vs. b for $a = 0.2, 1$ and 2 . The parameters $d = 0.1$ and $w = 2$.

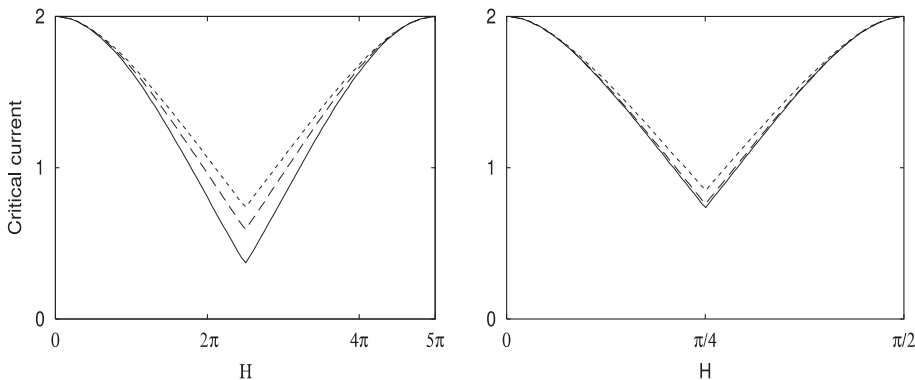


Fig. 13. Plot of $I_{\max}(H)$ for a large width of the passive region $w = 5$ and three values of b , $b = 0$ (continuous line), 1 (long dashed line) and 2 (short dashed line). The left panel corresponds to $a = 0.2$ and the right panel to $a = 2$. The parameter $d = 0.1$.

$a = 2$ the minimum critical current does not vary as b increases from 0 to 1. Only for $b = 2$ do we see an increase of the minimum critical current. This corresponds to the fact that p is almost flat in Fig. 12 for $a = 2$ and increases only for $b \approx w/2$.

5. Conclusions

We have analyzed the static behavior of two strip junctions in a 2D microstrip using a delta function approach. We establish that the problem can be reduced to a 1D effective one with a rescaled width \bar{w} which reflects the role of the surrounding region. For a small width only the fundamental transversal mode contributes to the solution so that $\bar{w} \approx w$ and the problem is close to unidimensional. For a large width many more transversal modes contribute making the problem essentially two dimensional, in that case $\bar{w} \gg w$ and $I_{\max}(H)$ changes significantly from the 1D estimate.

An important consequence of the rescaling is that the periodicity of the $I_{\max}(H)$ curve is equal to $\frac{\pi}{a}$ independently of the alignment of the junctions with respect to the magnetic field H . The analysis of the 1D effective problem also reveals that the minimum critical current is a/w for small a and increases slowly to its saturation as $a/w > 2$. The main effect of the 2D environment is to change this minimum critical current. For small a and large w it increases strongly to saturate and the $I_{\max}(H)$ curve becomes almost flat. The same happens when the mis-alignment b of the junction pair is increased and the effect is maximal for small a and large w .

We hope with this study to provide ways for experimentalists to tailor $I_{\max}(H)$ to suit specific needs. In particular they could adjust the curve to obtain maximum sensitivity in a specific region of field by placing the value of H giving the minimum critical current.

In the future we plan to tackle the problem of a larger number of junctions and compare to what is known for long junctions. One can also extend this modeling approach to other fields where one can have nonlinear inclusions.

Acknowledgements

The authors have benefitted from a French Ukrainian CNRS collaboration grant in 2000–2001 and a French–German Procope bi-lateral grant (04555 TG/02) in 2002–2003. Yuri Gaididei thanks the INSA de Rouen for its hospitality during his visit in March 2003. J.G. Caputo thanks Morvan Salez for useful discussions. Finally the authors are grateful to an anonymous referee for his careful reading and insightful remarks.

Appendix A. Reduction of the 2D problem

The first step is to solve the equation for A_m . For that we use the Green's function for the Helmholtz equation

$$(\partial_x^2 - k^2)G = -\delta(x - t), \quad (\text{A.1})$$

with the boundary condition $G|_{\pm\infty} = 0$. The Green function is

$$G(x, t) = \frac{1}{2k} \exp(-k|x - t|). \quad (\text{A.2})$$

This is strictly valid for an infinite domain in x but it can be shown that as soon as $l > 1$ it is a good approximation to the solution.

We introduce $A = A_0 + C$ and obtain A_m as

$$\begin{aligned} A_m = & -\frac{1}{m\pi} \left[\cos(m_-) \int_{-\infty}^{+\infty} dt g(t - a) \right. \\ & \times \sin(A + B_-(a)) e^{-\frac{m_-}{2}|x-t|} + \cos(m_+) \int_{-\infty}^{+\infty} dt g(t + a) \\ & \left. \times \sin(A + B_+(-a)) e^{-\frac{m_+}{2}|x-t|} \right], \end{aligned}$$

so that the functions $B_{\pm}(x)$ satisfy the following relations:

$$\begin{aligned} B_- \equiv & \sum_{m=1}^{\infty} A_m \cos(m_-) \\ = & -\frac{1}{\pi} \left[\int_{-\infty}^{+\infty} dt g(t - a) \sin(A + B_-(a)) C_{--} \right. \\ & \left. + \int_{-\infty}^{+\infty} dt g(t + a) \sin(A + B_+(-a)) C_{-+} \right], \end{aligned}$$

$$B_+ \equiv \sum_{m=1}^{\infty} A_m \cos m_+ \\ = -\frac{1}{\pi} \left[\int_{-\infty}^{+\infty} dt g(t-a) \sin(A+B_-(a)) C_{-+} \right. \\ \left. + \int_{-\infty}^{+\infty} dt g(t+a) \sin(A+B_+(-a)) C_{++} \right],$$

where we have introduced

$$C_{\pm\pm} = \sum_{m=1}^{\infty} \cos(m_{\pm}) \cos(m_{\pm}) \frac{e^{-\frac{\gamma m}{2}|x-t|}}{m}.$$

From these equations it is clear that we need the quantities $B_-(a)$ and $B_+(-a)$. We introduce the functions p and q such that

$$B_-(a) = -\frac{1}{2\pi} [p \sin(A(a) + B_-(a)) + q(a) \\ \times \sin(A(-a) + B_+(-a))], \quad (\text{A.3})$$

$$B_+(-a) = -\frac{1}{2\pi} [q(a) \sin(A(a) + B_-(a)) \\ + p \sin(A(-a) + B_+(-a))], \quad (\text{A.4})$$

so that

$$p = \int_{-\infty}^{+\infty} dt g(t) \sum_{m=1}^{\infty} \frac{e^{-\frac{\gamma m}{2}|t|}}{m} [1 + (-1)^m \cos(\gamma mb)], \quad (\text{A.5})$$

$$q(a) = \int_{-\infty}^{+\infty} dt g(t+a) \sum_{m=1}^{\infty} \frac{e^{-\frac{\gamma m}{2}|t-a|}}{m} (-1)^m \\ \times [1 + (-1)^m \cos(\gamma mb)]. \quad (\text{A.6})$$

Notice that p is independent of a and corresponds to a self-energy of the junction, in solid state physics, an on-site term. On the contrary q depends on a , the distance between the two junctions and corresponds to an interaction between them.

In the equation for A the function g in front of the sine terms can now be replaced by the Dirac delta function in x since in the 1D case there is no singularity for the Green's function

$$A_{xx} = \frac{1}{w} [\delta(x-a) \sin(A(a) + B_-(a)) \\ + \delta(x+a) \sin(A(-a) + B_+(-a))] - \eta \frac{I}{s}, \quad (\text{A.7})$$

with boundary conditions $A|_{x=\pm\frac{l}{2}} = H \pm (1-\eta) \frac{I}{2w}$.

We then have the following form for A , for $x < -a$, $A(x) = \alpha_- + \beta_- x - \eta \frac{I}{s} \frac{x^2}{2}$ while for $x > a$, $A(x) = \alpha_+ + \beta_+ x - \eta \frac{I}{s} \frac{x^2}{2}$.

The boundary conditions imply $\beta_{\pm} = H \pm \frac{I}{2w}$. For $-a < x < a$, $A(x) = \alpha_0 + \beta_0 x - \eta \frac{I}{s} \frac{x^2}{2}$. For $x = \pm a$ we have the following jump conditions for the derivative A_x so that

$$\beta_+ - \beta_0 = \frac{1}{w} \sin(A(a) + B_-(a)), \quad (\text{A.8}) \\ \beta_0 - \beta_- = \frac{1}{w} \sin(A(-a) + B_+(-a)).$$

Adding and subtracting these relations gives

$$I = 2 \sin \left(\frac{A(a) + A(-a) + B_-(a) + B_+(-a)}{2} \right) \\ \times \cos \left(\frac{A(a) - A(-a) + B_-(a) - B_+(-a)}{2} \right), \quad (\text{A.9})$$

$$H - \beta_0 = \frac{1}{w} \sin \left(\frac{A(a) - A(-a) + B_-(a) - B_+(-a)}{2} \right) \\ \times \cos \left(\frac{A(a) + A(-a) + B_-(a) + B_+(-a)}{2} \right). \quad (\text{A.10})$$

From the definitions of p and q ((A.5) and (A.6)) it can be seen that

$$B_+(-a) + B_-(a) = -\frac{I}{2\pi} [p + q(a)] \quad (\text{A.11})$$

and

$$B_+(-a) - B_-(a) = \frac{\gamma}{2} (H - \beta_0) [p - q(a)]. \quad (\text{A.12})$$

We now use the fact that A is continuous at $x = \pm a$ to obtain

$$\frac{1}{2} (A(a) + A(-a)) = \alpha_0 - \eta \frac{I}{s} \frac{a^2}{2} \quad (\text{A.13})$$

and

$$\frac{1}{2} (A(a) - A(-a)) = \beta_0 a. \quad (\text{A.14})$$

We now substitute the above four relations (A.11)–(A.14) into Eqs. (A.9) and (A.10) and get the system

$$\begin{aligned} I &= 2 \sin(\alpha) \cos(\beta a), \\ H - \beta_0 &= \frac{1}{w} \cos(\alpha) \sin(\beta a), \end{aligned} \quad (\text{A.15})$$

where

$$\begin{aligned} \alpha &\equiv \alpha_0 - \frac{I}{2} \left(\eta \frac{a^2}{s} + \frac{p + q(a)}{2\pi} \right) \quad \text{and} \\ \beta a &\equiv \beta_0 a - \frac{1}{\gamma} (p - q(a))(H - \beta_0). \end{aligned} \quad (\text{A.16})$$

We introduce the effective width \bar{w} and the 2D rescaling coefficient k as

$$\bar{w} = \frac{w}{k}, \quad k = 1 + \frac{w}{2\pi a} [p - q(a)] \quad (\text{A.17})$$

and obtain the system for α, β in its final form

$$\begin{aligned} I &= 2 \sin(\alpha) \cos(\beta a), \\ H - \beta &= \frac{1}{\bar{w}} \cos(\alpha) \sin(\beta a). \end{aligned} \quad (\text{A.18})$$

The expressions for $q(a)$ and p are computed in Appendix B.

Appendix B. Computation of $q(a)$ and p

From its definition $q(a)$ can be written as

$$\begin{aligned} q(a) &= \text{Re} \left\{ \int_{-\infty}^{+\infty} dt \sum_{m=1}^{\infty} \frac{e^{im\pi - m\gamma a}}{m} \right. \\ &\quad \left. \times [1 + (-1)^m \cos(\gamma mb)] \right\}, \end{aligned} \quad (\text{B.1})$$

where Re defines the real part of the expression and where we have used the fact that $g(t+a)$ is the Dirac delta function.

The series can be summed leading to

$$\begin{aligned} q(a) &= \text{Re} \left[-\log(1 - e^{i\pi - \gamma a}) - \frac{1}{2} \log(1 - e^{-\gamma a + i\gamma b}) \right. \\ &\quad \left. \times (1 - e^{-\gamma a - i\gamma b}) \right]. \end{aligned}$$

It is then straightforward to obtain the final result

$$\begin{aligned} q(a) &= -\log(1 + e^{-\gamma a}) \\ &\quad - \frac{1}{2} \log[1 - 2e^{-\gamma a} \cos(\gamma b) + e^{-2\gamma a}]. \end{aligned} \quad (\text{B.2})$$

For p the same type of calculation can be done. Starting from the definition

$$\begin{aligned} p &= \frac{2}{\sqrt{\pi}d} \int_0^{\infty} dt e^{-\frac{t^2}{d^2}} \sum_{m=1}^{\infty} \frac{e^{-\frac{m}{2}|t|}}{m} \\ &\quad \times (1 + (-1)^m \cos(\gamma mb)). \end{aligned} \quad (\text{B.3})$$

The summation can be written as

$$S(t) = \text{Re} \sum_{m=1}^{\infty} \frac{e^{-m\frac{|t|}{2}} + e^{m[-\frac{|t|}{2} + i(\pi + \gamma b)]}}{m},$$

which can be calculated as previously to yield

$$\begin{aligned} S(t) &= -\log(1 - e^{-\frac{|t|}{2}}) \\ &\quad - \frac{1}{2} \log[1 + e^{-\gamma|t|} + 2e^{-\frac{\gamma}{2}|t|} \cos(\gamma b)]. \end{aligned}$$

This expression can then be plugged into the integral of (B.3) and using the change of variable $x = \frac{|t|}{2}$ we obtain

$$\begin{aligned} S(x) &= -\log(1 - e^{-x}) - 0.5 \\ &\quad \times \log[1 + e^{-2x} + 2e^{-x} \cos \gamma b] \end{aligned}$$

and

$$p = \frac{2}{\sqrt{\pi}} \frac{w}{\pi d} \int_0^{\infty} dx e^{-N^2 x^2} S(x), \quad (\text{B.4})$$

where $N^2 = \frac{w^2}{\pi^2 d^2}$. This integral cannot be calculated analytically but a good approximation can be obtained by expanding $S(x)$ for $x \approx 0$ since $w \gg d$ ($N \gg 1$). We get

$$S(x) \approx x - \log(x) - \log(2) - \log\left(\cos \frac{\gamma b}{2}\right),$$

so that the integrals can be computed and we obtain the final result

$$p \approx \frac{1}{2} C + \frac{\sqrt{\pi}d}{w} + \log \frac{w}{\pi d} - \log\left(\cos \frac{\pi b}{w}\right), \quad (\text{B.5})$$

where $C \approx 0.577216$ is the Euler constant [14].

References

- [1] K. Likharev, Dynamics of Josephson Junctions and Circuits, Gordon and Breach, 1986.
- [2] A. Barone, G. Paterno, Physics and Applications of the Josephson Effect, John Wiley, 1982.
- [3] J.G. Caputo, N. Flytzanis, M. Vavalis, Int. J. Mod. Phys. C 6 (2) (1995) 241.

- [4] A. Benabdallah, J.G. Caputo, N. Flytzanis, *Physica D* 161 (2002) 79.
- [5] C.S. Owen, D.J. Scalapino, *Phys. Rev.* 164 (1967) 538.
- [6] T.C. Chow, H. Chou, H.G. Lai, C.C. Liu, Y.S. Gou, *Physica C* 245 (1995) 143.
- [7] Yu.A. Gal'pern, T.V. Filippov, *Sov. Phys. JETP* 59 (1984) 894.
- [8] R. Fehrenbacher, V.B. Geshkenbein, G. Blatter, *Phys. Rev. B* 45 (1992) 10.
- [9] J.G. Caputo, N. Flytzanis, A. Tersenov, M. Vavalis, *SIAM J. Math. Anal.* 34 (2003) 1356.
- [10] J.G. Caputo, N. Flytzanis, M. Vavalis, *Int. J. Mod. Phys. C* 7 (1996) 191.
- [11] A. Franz, A. Wallraff, A.V. Ustinov, *J. Appl. Phys.* 89 (2001) 471.
- [12] M.H. Chung, M. Salez, in: *Proceedings of the 4th European Conference on Applied Superconductivity, EUCAS 99*, 651, 1999.
- [13] T. Van Duzer, C.W. Turner, *Principles of Superconducting Devices and Circuits*, Edward Arnold, 1985.
- [14] I.S. Gradstein, I.M. Ryzhik, *Tables of Integrals, Series and Products*, Academic Press, 1980.